# Transport gap renormalization at a metal-molecule interface using DFT-NEGF and spin unrestricted calculations

Celis Gil, J. A.; Thijssen, J. M.

# Transport gap renormalization at a metal-molecule interface using DFT-NEGF and spin unrestricted calculations

J. A. Celis Gil, and J. M. Thijssen

## Articles you may be interested in

Pair 2-electron reduced density matrix theory using localized orbitals
The Journal of Chemical Physics 147, 084101 (2017); 10.1063/1.4999423

The nature of three-body interactions in DFT: Exchange and polarization effects
The Journal of Chemical Physics 147, 084106 (2017); 10.1063/1.4986291

Efficient algorithms for large-scale quantum transport calculations
The Journal of Chemical Physics 147, 074116 (2017); 10.1063/1.4998421

Vibrational relaxation beyond the linear damping limit in two-dimensional optical spectra of molecular aggregates
The Journal of Chemical Physics 147, 084104 (2017); 10.1063/1.4999680

Neural network based coupled diabatic potential energy surfaces for reactive scattering
The Journal of Chemical Physics 147, 084105 (2017); 10.1063/1.4997995

Non-renewal statistics for electron transport in a molecular junction with electron-vibration interaction
The Journal of Chemical Physics 147, 104109 (2017); 10.1063/1.4991038

AIP | The Journal of Chemical Physics

PERSPECTIVES

# Transport gap renormalization at a metal-molecule interface using DFT-NEGF and spin unrestricted calculations

J. A. Celis Gil and J. M. Thijssen
*Kavli Institute of Nanoscience, Delft University of Technology, 2628 CJ Delft, The Netherlands*

A method is presented for predicting one-particle energies for a molecule in a junction with one metal electrode, using density functional theory methods. In contrast to previous studies, in which restricted spin configurations were analyzed, we take spin polarization into account. Furthermore, in addition to junctions in which the molecule is weakly coupled, our method is also capable of describing junctions in which the molecule is chemisorbed to the metal contact. We implemented a fully self-consistent scissor operator to correct the highest occupied molecular orbital-lowest unoccupied molecular orbital gap in transport calculations for single molecule junctions. We present results for various systems and compare our results with those obtained by other groups. *Published by AIP Publishing.* [http://dx.doi.org/10.1063/1.4999469]

## I. INTRODUCTION

A major issue in calculations of molecular electronics devices is the alignment of molecular orbital levels relative to the Fermi energy of the metal electrodes.

In the gas phase, molecules have well defined energy levels, two of which relate to the orbitals that play a major role in charge transport: the highest occupied molecular orbital (HOMO) and the lowest unoccupied molecular orbital (LUMO).

According to Koopmans' theorem, within the Hartree Fock approximation, the energy needed to remove one electron from an isolated molecule, known as Ionization Potential (IP), is equal to the energy difference between the HOMO and the vacuum level.[1,2] Similarly, the Electron Affinity (EA), which is the energy needed to put an extra electron into the molecule, is the energy difference between the LUMO and the vacuum level. Koopmans theorem predicts the HOMO and LUMO levels in Hartree-Fock reasonably well. When the molecule is close to a metal surface, the molecular energy levels shift, due to various reasons, such as image charge formation and a modification of the interface dipole.[3–6]

In density functional theory (DFT), Janack's theorem predicts the HOMO in an analogous way, but there, orbital relaxation effects make this theorem unusable in small systems or large systems with weak polarization.[7–10]

It has been demonstrated experimentally that the vicinity of a metal electrode leads to a reduction of the gap between the ionization potential and electron affinity of a molecule with respect to that of the gas phase.[11–14] The reduction of the IP and EA of the molecule is mainly due to the Coulomb interaction between the added charge on the molecule and the screening electrons in the leads. This feature, called the image-charge effect,[4,5,15–17] becomes more relevant as the molecule gets closer to the metallic surface.

In standard DFT, approximations for the exchange and correlation potentials, which are widely used in transport calculations, do not account for the nonlocal correlation effects responsible of the adjustment of the frontier levels.[18–21]

One way to include these non-local effects is to use the GW approximation constructed on top of DFT.[22–24] This approach has successfully predicted level alignment.[15,25–30] However the GW scheme is very expensive computationally, which limits the size of the system that can be analyzed within this scheme, especially in a junction, which includes many lead atoms.

In the weak coupling regime, other methods like constrained density functional theory (CDFT) and density functional theory together with non-equilibrium Green's function (DFT-NEGF) technique have been implemented to analyze the level alignment at the interfaces.[17,31–33]

In the work presented by Souza *et al.*,[31] CDFT is used to determine the charge-transfer energy of a molecule physisorbed on a metallic surface. This method gives quantitatively accurate results at small molecule-metal separations; however, in order to obtain quantitatively converged results, large metal cluster sizes are needed for large distances, and metal atoms with a few valence electrons must be used in order to keep the calculations manageable.

Using classical electrodynamics, it is possible to predict the level shifts close to a metallic surface.[4,5,15–17] In a previous paper, we calculated the energy level adjustment of a molecule in the junction caused by image-charge effects using classical electrostatics.[17] Atomic charges for the molecule in the junction (from a NEGF-DFT calculation) rather than in the gas phase were used for the image-charge calculation. In this way, features that are absent in the gas phase are included. First, with the formation of interface levels, the relevant charge states of the molecule have a different character in the gas phase than in a junction; and second, the reference state in the junction (at zero bias and gate) can carry a net charge, which implies a significant contribution to the reduction of the metal work function upon chemisorption of a molecule. However, with this approximation, only the level *shifts* are calculated but

**147**, 084102-1

the values of the IP, EA, and EA-IP gap cannot be calculated explicitly.

Another method, introduced by Stadler et al.,[32,33] makes use of the NEGF formalism and calculates the addition energy for single molecule junctions in the Coulomb blockade regime. This method puts less severe restrictions on the kind of atoms that can be used for the leads than the Souza's approach. However, in this work, the input energy required for the transfer of one electron from the molecule to the electrodes or vice versa in terms of the external potential was calculated without taking into account anchoring groups, hence partial charge transfer cannot be accounted for. The results are therefore not directly applicable to experimental transport junctions with chemisorbed molecules. Stadler's method uses the electrostatic energy calculated in the transport code—no classical electrostatic calculation is needed.

In the present paper, we adapt the method introduced by Stadler et al. to explicitly calculate the IP and the EA of a molecule close to a metallic electrode. We perform spin unrestricted calculations varying the gate voltage and we obtain the charge state of the molecule for every gate. To determine the energy needed to add/remove one electron, we take into account the partial charge transfer between molecule and lead. Initially, we consider a benzene ring, which is a standard molecule for this kind of calculations, and then we show that our method is valid even if we take into account anchoring groups and short molecule-metal separations. Additionally we implemented the CDFT method to speed up the process. In our implementation into the transport module of ADF-BAND, the determination of the potential shift in the CDFT method is automated for efficiency, in this way the location of the ionization and addition level are accurately determined. The DFT eigenvalues corresponding to the occupied and unoccupied levels can be shifted to those values by means of a scissors operator (SOC) such that the transmission through the junction is corrected, improving the conductance value when compared with experimental data.

In Sec. III, we shall apply our method to a benzene ring, which is a standard molecule for this type of calculation in front of a metallic lead. We use two different materials for the lead and we compare our results with those obtained by others. In Sec. IV, we include anchoring groups and we apply our method to the 1,4 benzenediamine (BDA) molecule. We compare our results with those predicted by an electrostatic calculation of image charge effect. In Sec. V, we extend our method to a single molecule junction formed by a 1,4 benzenediamine molecule connected to two gold electrodes. Then we apply a fully self-consistent field (SCF) scissors operator to correct the transmission through the molecular junction.

## II. MODEL

One of the most used experimental techniques for molecular devices is the mechanically controlled break junction (MCBJ). In this technique, a wire is suspended on top of a substrate that can bend. The bending results in stretching of the top wire which may break and form a nano-gap. We adapt

the model implemented by Verzijl and Thijssen[34] to analyze the level alignment of a molecule in front of the nanowire and we perform spin unrestricted calculations[35] in the DFT-NEGF scheme.

We locate a planar molecule at a distance $d$ in front of the surface of a nanowire. The distance $d$ is the smallest distance measured from the centers of the atoms in the molecule to the lead surface (see Figs. 1 and 5). We apply a gate potential, which is constant across the molecule, with the molecule defined as all the non-metallic atoms. The gate is applied to the orbitals of the electrons of the molecule (see the supplementary material of Ref. 17) and we obtain the electronic configuration of the system after the self-consistent procedure within the DFT-NEGF framework.

When the peak of the broadened levels aligns with the electrode's Fermi level, half of that level is occupied so that the gate needed to remove half electron from the molecule corresponds to $IP_{mol}$ and the gate needed to add half corresponds to $EA_{mol}$.[32]

We analyze the spin resolved occupation of the molecule, which indicates how the filling of the individual levels changes upon varying the gate. Because of its nature as spatial decompositions, we prefer to use the spin-projected Hirshfeld charge decompositions rather than the basis-set decompositions like Mulliken.

Depending on the coupling strength between the molecule and the lead ($\Gamma$) with respect to the quantum splitting and the Coulomb repulsion for electrons at the relevant level ($U$), we distinguish three regimes (see Fig. 2). (i) Uncoupled ($\Gamma = 0$),
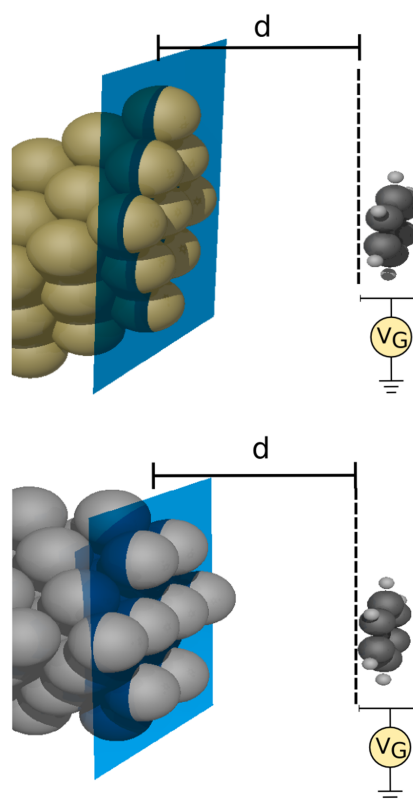


FIG. 1. Cases studied with a benzene molecule parallel to a gold 111 plane (top) and a lithium 100 plane (bottom) lead surface. We show how we define the distance $d$ and the gate applied over the molecule.
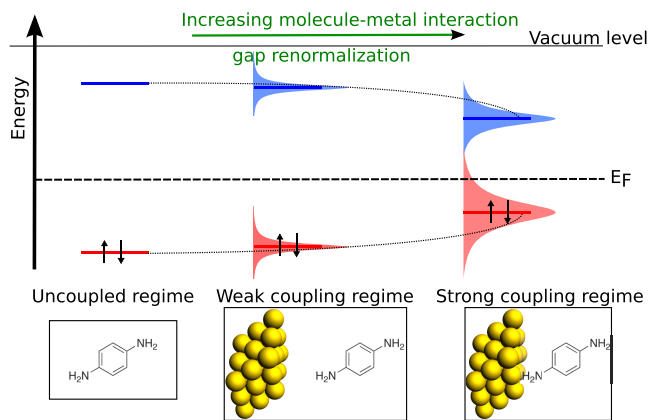
FIG. 2. Schematic drawing of the molecular orbitals with respect to the Fermi energy ($E_F$). (Left) Isolated molecule. (Middle) The molecule interacts with the metal lead only via long-range interactions. (Right) Chemical bonds between the molecule and the lead.

(ii) the molecule and the lead are weakly coupled ($\Gamma < \Delta E$), and (iii) the molecule is strongly coupled to the lead ($\Gamma > \Delta E$). With $\Delta E$ the level splitting.

In the uncoupled regime, there is no partial charge transfer or broadening of the molecular energy levels which remain sharply defined. This regime appears when the molecule is very far from the electrode.

In the weak coupling regime, we have some broadening of the molecular energy levels. In the uncoupled and weakly coupled regimes, at zero gate, the molecule has approximately an integer number of electrons and spin equal to $\frac{1}{2}$ or 0, hence the spin resolved charge form plateaus and present spin polarization when viewed as a function of the gate.

At large molecule-electrode separations, we would expect plateaus in the occupation of the different levels versus gate voltage. However, in DFT, such plateaus do not occur, even for an isolated molecule. This is due to the absence of the derivative discontinuity in the local functional used.[36] However, it has been pointed out by several researchers that the spin-polarized states found in DFT calculations can give valuable information about the many-body resonances of the spectral density.[37–40]

Finally, in the strong coupling regime, the lead and the molecule are connected, leading to charge transfer across the interface, even at zero bias and gate,[41] which contributes to the reduction of the EA-IP gap. The charge excess in the molecule is calculated with respect to the neutral state of the isolated molecule.[17]

In the first two regimes, as the partial charge transfer at zero gate is very small, the molecule is expected to be neutral. This simplifies the process to determine the IP and EA. We determine the gate that we need in order to add or remove half integer charge to or from the molecule in the reference configuration (zero bias and gate) using our implementation of a CDFT method into the DFT-NEGF framework.

In CDFT, the minimum of the energy functional is searched under the constraint that the charge, which is calculated as

$$N_{added} = \int_{molecule} n(\mathbf{r})\, d^3 r, \qquad (1)$$

has a predefined value.

The constraint is realized through a Lagrange parameter $V$, which translates into a gate potential applied to the molecule.[42–44] This extra potential is equivalent to a constant gate voltage and has been implemented in our transport code. We also implement an automated algorithm for finding the gate which gives a desired charge. This implementation reduces the cpu time substantially.

It is important to emphasize that there is no classical image charge effect calculation performed—the image charge effect is fully accounted for by the Hartree potential calculation done by DFT. The fact that the self-energy keeps the part of the contact not facing the molecule neutral is crucial for this.

## III. BENZENE

We first consider a benzene molecule, with its plane parallel to the electrode surface. We use two different metal leads, Au and Li. Au is frequently used in experiments and Li allows us to compare our results with those obtained by Souza et al.[31] for the same system. Additionally, we compare the effects on the level alignment for both lead materials.

For the gold lead, we use a scattering region that contains 27 atoms arranged in a FCC lattice, whereas for the Li lead, the scattering region contains 32 atoms arranged in a BCC lattice. All the metal atoms are fixed at the crystal lattice positions. For Au, the lattice constant is 4.0782 Å and for Li 3.51 Å. In both cases, we do not consider periodic boundary conditions parallel to the surface of the electrode and there is no chemisorption between the surfaces and the molecule.

For our calculations, we use a DZP-basis of numerical atomic orbitals on the molecule, a SZ-basis of numerical atomic orbitals on the gold atoms, a DZ-basis of numerical atomic orbitals on the lithium atoms and the Perdew, Burke, and Ernzerhof (PBE) parametrization of the Generalized Gradient Approximation (GGA) functional in our implementation of NEGF-based transport in the Amsterdam Density Functional (ADF)/band quantum chemistry package.[34,45,46]

Figure 3 shows the spin-resolved number of electrons on the molecule which is placed in front of a gold/lithium lead as a function of the applied gate for $d = 2$ Å, $d = 6$ Å, and $d = 14$ Å. We observe plateaus around zero gate corresponding to the (almost) neutral state, except for the chemisorbed molecules (2 Å), as expected.

For short separation, for zero gate, we observe a charge, close, but not exactly equal to zero. This charge is due to interfacial charge transfer; there is no spin polarization. Changing the gate towards negative values, the spin polarization is still absent, whereas positive gate voltages quickly lead to splitting of the charge across the two spins. These configurations regularly switch to spin-polarized ones and back. Furthermore, the average curve shows an inflection close to zero gate voltage.

To determine the IP and EA, we identify the spin polarized plateau close to the neutral configuration. This plateau determines the background charge state of the molecule. Then, we
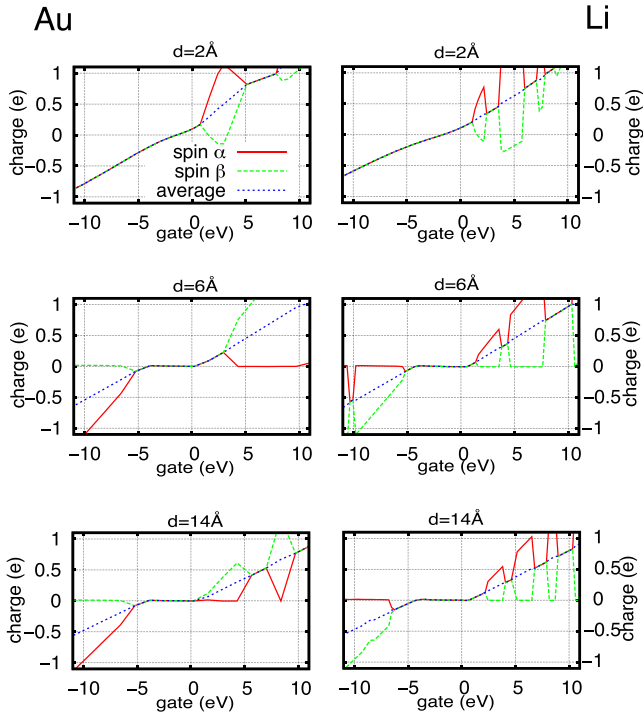
FIG. 3. Hirshfeld spin-resolved number of electrons in the benzene as a function of the applied gate for a distance equal to 2 Å, 6 Å, and 14 Å between the lead and the molecule, using a Au lead (left) and a Li lead (right). Positive values in the charge mean that electrons have been removed from the molecule.

look for the gate needed to remove/add half charge (IP/EA) with respect to the background.

In the case of larger separations, the background charge state coincides with zero charge excess as partial charge transfer at zero gate is absent.

In the uncoupled regime, the polarization is less constant than in the weak coupling regime, and the system switches between non-polarized charge and polarized charge.

Comparing the charge occupations for the different separations (Fig. 3), the presence of polarization is more common in the weak coupling condition $\Gamma < \Delta E$. Polarization should not occur or be less present when $\Gamma > \Delta E$. This appears to be the case when the molecule is close to the lead. Independent of the regime, the spin polarization is more common to switch on when the total charge excess in the molecule is a multiple integer of 0.5 $e$, it means just after an energy peak of the molecule is aligned with the electrode's Fermi
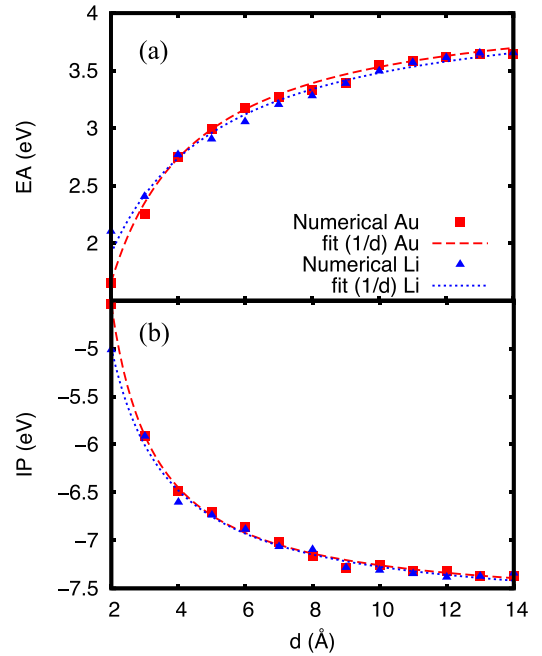


FIG. 4. Ionization potential and electron affinity calculated in eV as a function of the distance between the benzene and the lead in (Å) using (a) a gold lead and (b) lithium lead.

energy. Whereas the charge excess for one of the spins stays constant, the other one changes, which indicates, as we established in Sec. II, that only one type of spin is added to or removed from the system. However, for this case of a benzene ring facing a lead in a parallel position, the behavior is rather switchy and it does always show clear plateaus, probably because of the absence of a derivative discontinuity in the XC potential.

In Fig. 4 we show the IP and EA as a function of the distance between the lead and the molecule for the two different metals used.

We fit our data using the electrostatic energy of a point charge $q$ located in vacuum at a distance $d$ in front of a semi-infinite conductor given by

$$V = \frac{qq'}{4d}. \tag{2}$$

We see that our method reproduces the image charge effect well. Furthermore, the differences between the two lead materials considered are small.

With a lithium lead, the image-charge plane that we obtained from our fits is $1.32 \pm 0.06$ Å and $1.41 \pm 0.05$ Å for

TABLE I. Comparison of benzene IP and EA. The first column shows the EA/IP obtained using our method with the molecule in front of two different metallic leads in the limit of large distances. The next two columns show the results obtained by Stadler et al.[33] and Souza et al.,[31] respectively. Then the "Gas phase" column shows the results obtained by Hartree-Fock, ΔSCF, and GW[26] methods. In the last column, we show the experimental results reported in Refs. 47 and 48.

| | Present work | | Stadler | Souza | Gas phase | | | Experimental |
|---|---|---|---|---|---|---|---|---|
| | Au | Li | Al | Li | HF | ΔSCF | GW | |
| IP (eV) | $7.70 \pm 0.03$ | $7.77 \pm 0.06$ | ... | 7.38 | 9.64 | 9.74 | 7.9 | 9.4[47] |
| EA (eV) | $4.14 \pm 0.05$ | $4.15 \pm 0.07$ | ... | 4.89 | 3.18 | 1.50 | 2.7 | 1.1[48] |
| Gap (eV) | $11.84 \pm 0.08$ | $11.92 \pm 0.13$ | 11.54 | 12.27 | 12.82 | 11.24 | 10.6 | 10.5 |

the IP and the EA, respectively. These values are in good agreement with the results obtained by Garcia-Lastra et al.[26] of 1.62 Å and Souza et al.[31] of 1.72 Å for EA and 1.80 Å for IP. The values obtained with a gold lead are $0.68 \pm 0.07$ Å for the IP and $0.58 \pm 0.09$ Å for the EA. In general, the values obtained for the image-plane with gold are smaller; we attribute this effect to the higher electronic density of gold close to the surface.

In our calculations and fits, we find that the values for the image-charge plane obtained are in general different for occupied and unoccupied energy levels. This is because the shape of the molecular orbitals also affects the size of the polarization giving as a result different behaviors in every case. We will return to this point with the BDA molecule in Sec. IV.

In Table I, we compare our results for the IP and EA with those obtained using other methods for gas phase ΔSCF, Hartree-Fock, and GW[26] and methods that consider metallic surfaces like DFT-NEGF and CDFT. We can see that our results are in good agreement with those obtained by other authors.

## IV. 1,4 BENZENEDIAMINE (BDA)

We now proceed to a system in which covalent bonds may occur, due to anchoring groups at the ends of the molecule. In this case, the molecule has a different orientation with respect to the lead.

We put a 1,4 BDA molecule in front of the lead with the carbon atoms plane perpendicular to the lead surface. One of the amine groups of the molecule is located at a distance $d$ from the electrode (Fig. 5). For this molecule, we use a DZP-basis of numerical atomic orbitals and the GGA functional.

Spin polarization is more prominent in this case as compared to the previous case (Fig. 6). This is probably due to the fact that only few basis orbitals (of the amine group) couple to gold instead of all the $p_z$ orbitals of the carbon atoms in the previous case. This prominence of the plateaus makes it easier to identify the charge states in the weakly coupled and uncoupled cases than for the parallel configuration. It is important to note that the short distance configuration for benzene is artificial given that 2 Å is a distance shorter than the equilibrium position of the molecule over a substrate.

Our calculations show that image-charge effects contribute significantly to the distance-dependent renormalization of the molecular orbital levels with respect to the Fermi level of the electrode (Fig. 7). For short distances, the energy values for the IP and the EA are different for the gold lead and the lithium lead. We attribute this difference to the anchoring group which is responsible for creating a bond between the lead and the molecule.

The values for the IP obtained in the long distance limit ($d \to \infty$) are $3.19 \pm 0.13$ eV and $3.20 \pm 0.05$ eV for gold and lithium, respectively, and the EA values are $6.36 \pm 0.07$ eV for gold and $6.42 \pm 0.08$ eV for lithium. At this limit, the EA-IP gap obtained is very similar for both materials.

Comparing our results with those obtained previously by us,[17] where the image charge effect for the same molecule is analyzed using a separate classical approximation based on atomic point charges, we observe similar asymmetric trends for the EA and the IP as a function of the distance. This effect is mainly due to the resident charge in the molecule and becomes more relevant for short distances.
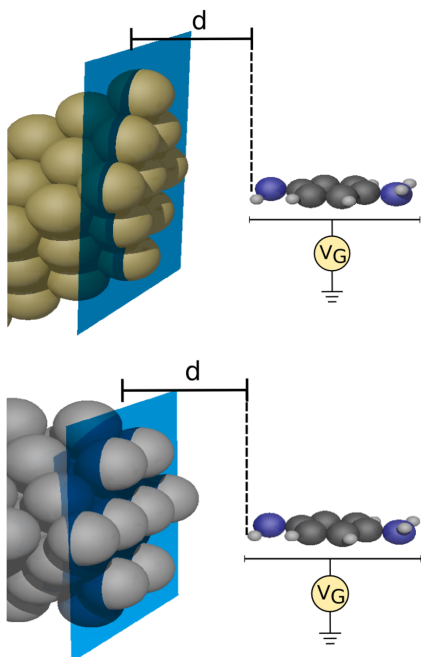


FIG. 5. Scheme showing the 1,4 BDA molecule in front of the gold 111 plane (top) and lithium 100 plane (bottom) lead surface. We show how we define the distance $d$ and the gate applied on the molecule for every lead.
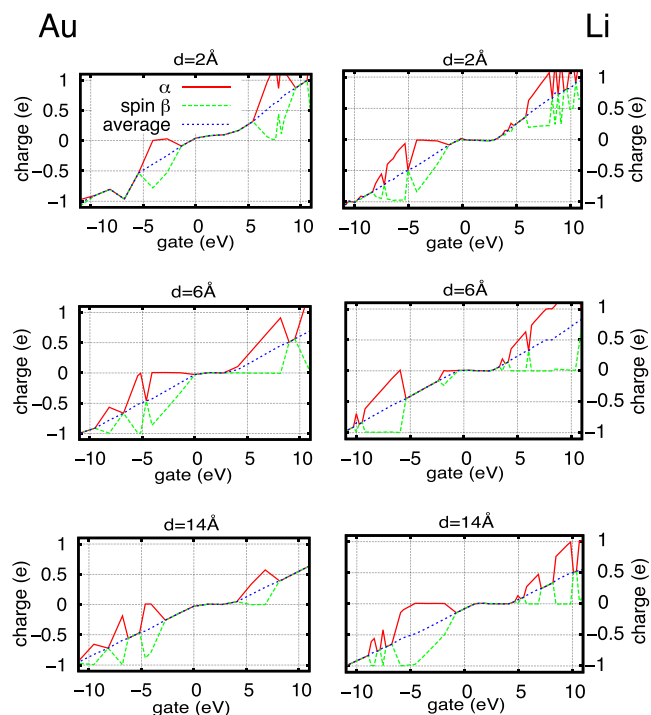


FIG. 6. Spin resolved Hirshfeld number of electrons in the 1,4 BDA as a function of the applied gate for a distance equal to 2 Å, 6 Å, and 14 Å between the lead and the molecule, using a Au lead (left) and a Li lead (right).
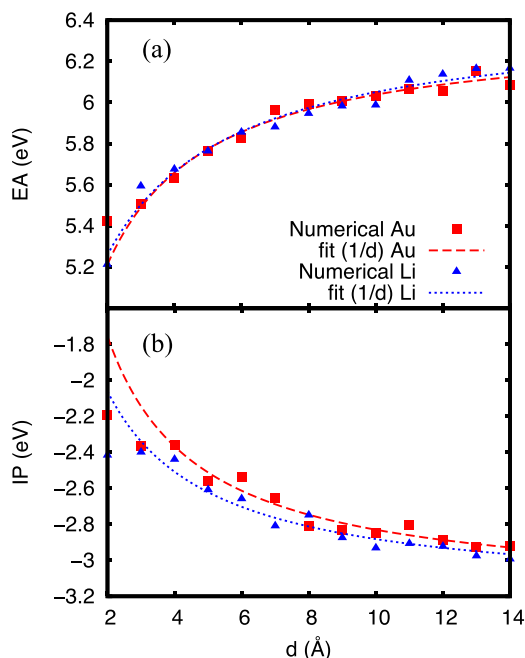
FIG. 7. Ionization potential and electron affinity calculated in eV as a function of the distance between the 1,4 BDA and the lead in (Å) using (a) gold lead and (b) lithium lead.

Finally, at the distance where the formation of the chemical bond occurs, we observe a deviation of the calculated levels from the $\frac{1}{d}$ behavior. This occurs for $d$ between 2 and 3 Å.

## V. AU-BDA-AU JUNCTION AND SCISSORS OPERATOR

In Sec. IV, we considered the molecular level alignment of a molecule near a metal surface, we now extend our model to a single molecule junction, in which we consider a 1,4 BDA molecule in between two gold electrodes. We consider a junction of type (I,I) according to Quek *et al.*[3] (see Fig. 8).

For the molecule in the junction, we relax the geometry. We then apply a gate over the molecule in order to find the IP and EA values. The molecule in the junction, at zero gate for the relaxed geometry, has a positive charge of 0.274. We find that in order to remove one electron from the molecule, we have to apply a gate $-2.86$ eV and to put an extra electron corresponds to 3.82 eV (see Fig. 9). These values are in agreement with those presented in Sec. IV.
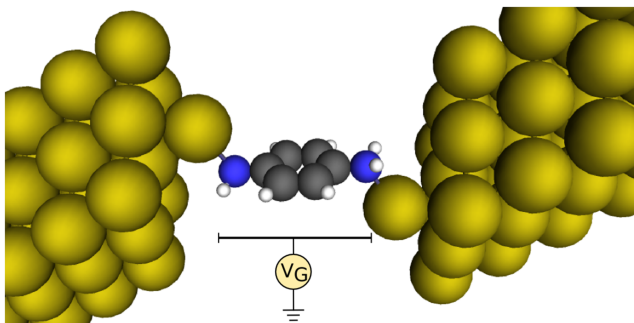


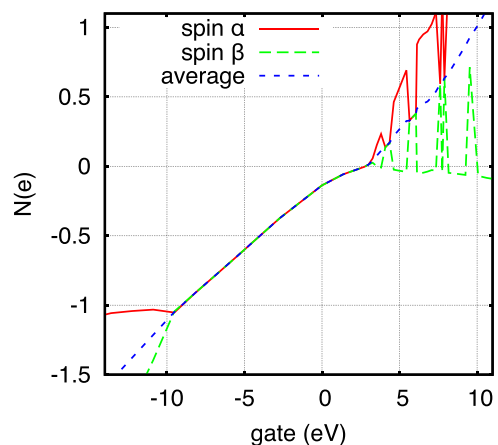FIG. 8. Scheme showing the Au-BDA-Au junction and the gate applied on the molecule.



FIG. 9. Number of electrons per spin in the molecule as a function of the applied gate.

Having a reliable value of the ionization and addition levels, we now shift the DFT eigenvalues of the molecule to the desired energies by means of a scissors operator (SCO)[3,4,49,50] that has been proven to improve the conductance compared with experimental results.[3] It should be emphasized that our procedure does not use gas-phase levels and corrections. Instead, our implementation directly uses values obtained from the molecule in the junction. First, the Hamiltonian and overlap matrix of the molecule ($H_{mol}^0$, $S_{mol}^0$) are extracted from the complete system, and we obtain their eigenvalues and eigenvectors. Then, the corrections are applied to the eigenvalues by shifting all the occupied levels down by a constant value $\phi_{occ}$, while the unoccupied levels are shifted up by $\phi_{unocc}$. With the shifted eigenvalues, the eigenvectors, and the overlap matrix, we calculate the scissors operator Hamiltonian ($H_{mol}^S$), which will replace the $H_{mol}^0$ in the full system Hamiltonian. The scissors operator procedure is applied in each cycle of the self-consistent DFT-NEGF procedure.

For our DFT-NEGF calculations, we use the same basis sets that we used in Secs. II–IV in addition to the GGA PBE functional. Once convergence is reached, the transmission is calculated. In the limit of zero bias, we obtain the zero bias conductance from the Fisher-Lee relationship $G = G_0 T(E_F)$. In terms of $G_0 = \frac{2e^2}{h}$ the conductance quantum, the conductance value with the SCO correction is $0.0082G_0$, which represents a significant reduction of one order of magnitude with respect to the value of $0.077G_0$ obtained without the SCO correction. This is in good agreement with the experimental conductance $0.0064G_0$ reported.[3,51,52]

Considering the molecule in the gas phase, the scissors operator can be applied to correct the transmission of the molecule attached to wide band electrodes, giving as a result a conductance equal to $0.007G_0$. However, with this approximation, the result is arbitrary given that the coupling strength is selected by hand to adjust the results.

It is important to remark that in our calculations as the IP and EA for the molecule are calculated in the junction, the scissors operator correction takes into account the image charge effect and the HOMO LUMO gap renormalization due to the presence of the electrodes (Fig. 10).
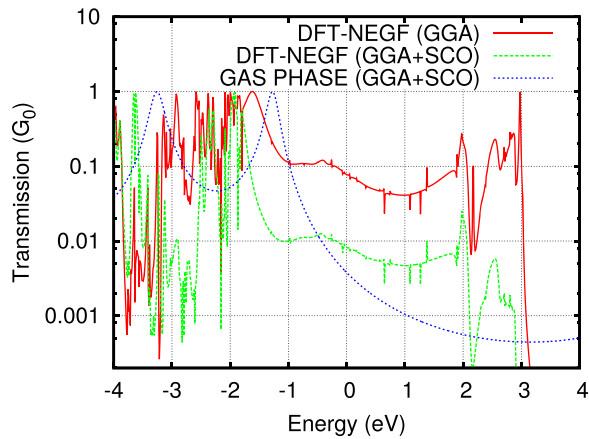
FIG. 10. Transmission coefficients as a function of the energy for the Au-BDA-Au junction using full SCF DFT-NEGF calculations without (dashed blue) and with (solid red) the scissor operator correction. The green dotted line was calculated for the molecules in the gas phase attached to wide band limit electrodes using $\Gamma = 0.5$.

## VI. CONCLUSIONS

In summary, we have presented a method where we use DFT-NEGF calculations together with spin unrestricted calculations that allow us to calculate the IP and the EA of a molecule in front of a metallic lead. Our method allows us to use different kinds of materials for the lead and predicts the IP-EA gap renormalization as a function of the distance between the lead and the molecule. With this method, it is possible to correct the position of the HOMO and LUMO peaks in the transmission curves of molecular junctions obtained using DFT-NEGF giving as a result a better agreement between experiments and calculations.

## ACKNOWLEDGMENTS

## APPENDIX: ANDERSON JUNCTION

In order to demonstrate how a spin-polarized calculation can reproduce resonances of the spectral density, for both spin directions, we have performed calculations for a simple model for a molecule, containing two energy levels, one level at $-\varepsilon_0$ and the other at $\varepsilon_0$ with respect to the chemical potential $\mu$. In the reference state (zero bias and gate), the lowest level is occupied by two electrons and the highest is empty.

We calculate the density within the Hartree approximation in which the potential for an electron at a level $i$ with spin $\sigma$ is shifted by $(U_{\sigma,\sigma*}n_{i\sigma*}) + \sum_{j\neq i,\sigma} \left(V_{ji}n_{j\sigma}\right)$, where $U_{\sigma,\sigma*}$ is the repulsion between two electrons in the same energy level and $V_{ji}$ the repulsion between two electrons in different energy levels and $\sigma* = -\sigma$. The occurrence of the $n_{j\sigma}$ implies that this should be done self-consistently with the possibility of having more than one stationary state.

The result for the occupation versus gate $V_g$ is shown in Fig. 11. The figure clearly shows that in the case where $U \gg \Gamma$, a spin splitting, similar to that observed in our DFT
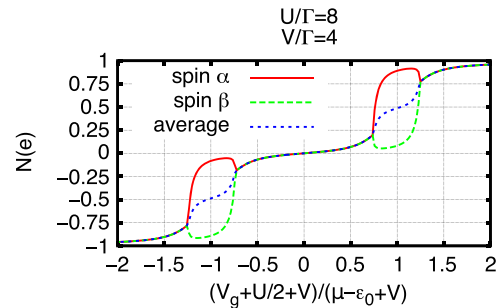


FIG. 11. Number of electrons added to the system per spin as a function of gate for the two-level system including the coulomb repulsion. With $V/\Gamma = 4.0$ and $U/\Gamma = 8.0$.

calculations, occurs. For $U \ll \Gamma$, this splitting disappears. The $V/\Gamma$ ratio does not affect the splitting occurrence. This splitting depends on the initial guess for the electron densities. If they are taken equal, the converged configuration does not always show spin splitting.

[1]P. Politzer and F. Abu-Awwad, Theor. Chem. Acc. **99**, 83 (1998).
[2]B. N. Plakhutin, E. V. Gorelik, and N. N. Breslavskaya, J. Chem. Phys. **125**, 204110 (2006).
[3]S. Y. Quek, L. Venkataraman, H. J. Choi, S. G. Louie, M. S. Hybertsen, and J. B. Neaton, Nano Lett. **7**(11), 3477 (2007).
[4]D. J. Mowbray, G. Jones, and K. S. Thygesen, J. Chem. Phys. **128**, 111103 (2008).
[5]K. Kaasbjerg and K. Flensberg, Nano Lett. **8**, 3809 (2008).
[6]H. Ishii, H. Oji, E. Ito, N. Hayashi, D. Yoshimura, and K. Seki, J. Lumin. **87-89**, 61 (2000).
[7]A. J. Cohen, P. Mori-Sánchez, and W. Yang, Phys. Rev. B **77**, 115123 (2008).
[8]A. J. Cohen, P. Mori-Sanchez, and W. Yang, Science **321**, 792 (2008).
[9]A. J. Cohen, P. Mori-Sánchez, and W. Yang, J. Chem. Phys. **129**, 121104 (2008).
[10]A. J. Cohen, P. Mori-Sánchez, and W. Yang, J. Chem. Phys. **126**, 191109 (2007).
[11]R. Hesper, L. H. Tjeng, and G. A. Sawatzky, Europhys. Lett. **40**, 177 (1997).
[12]J. Repp, G. Meyer, S. M. Stojković, A. Gourdon, and C. Joachim, Phys. Rev. Lett. **94**, 026803 (2005).
[13]M. T. Greiner, M. G. Helander, W.-M. Tang, Z.-B. Wang, J. Qiu, and Z.-H. Lu, Nat. Mater. **11**, 76 (2012).
[14]M. L. Perrin, C. J. O. Verzijl, C. A. Martin, A. J. Shaikh, R. Eelkema, H. van EschJan, J. M. van Ruitenbeek, J. M. Thijssen, H. S. J. van der Zant, and D. Dulic, Nat. Nanotechnol. **8**, 282 (2013).
[15]J. B. Neaton, M. S. Hybertsen, and S. G. Louie, Phys. Rev. Lett. **97**, 216405 (2006).
[16]K. Kaasbjerg and K. Flensberg, Phys. Rev. B **84**, 115457 (2011).
[17]C. J. O. Verzijl, J. A. Celis Gil, M. L. Perrin, D. Duli, H. S. J. van der Zant, and J. M. Thijssen, J. Chem. Phys. **143**, 174106 (2015).
[18]P. Hohenberg and W. Kohn, Phys. Rev. **136**, B864 (1964).
[19]W. Kohn and L. J. Sham, Phys. Rev. **140**, A1133 (1965).
[20]C. D. Pemmaraju, T. Archer, D. Sánchez-Portal, and S. Sanvito, Phys. Rev. B **75**, 045101 (2007).
[21]A. Filippetti, C. D. Pemmaraju, S. Sanvito, P. Delugas, D. Puggioni, and V. Fiorentini, Phys. Rev. B **84**, 195127 (2011).
[22]J. C. Inkson, J. Phys. C: Solid State Phys. **6**, 1350 (1973).
[23]M. S. Hybertsen and S. G. Louie, Phys. Rev. B **34**, 5390 (1986).
[24]G. Onida, L. Reining, and A. Rubio, Rev. Mod. Phys. **74**, 601 (2002).
[25]J. M. Garcia-Lastra and K. S. Thygesen, Phys. Rev. Lett. **106**, 187402 (2011).
[26]J. M. Garcia-Lastra, C. Rostgaard, A. Rubio, and K. S. Thygesen, Phys. Rev. B **80**, 245427 (2009).
[27]I. Tamblyn, P. Darancet, S. Y. Quek, S. A. Bonev, and J. B. Neaton, Phys. Rev. B **84**, 201402 (2011).
[28]G.-M. Rignanese, X. Blase, and S. G. Louie, Phys. Rev. Lett. **86**, 2110 (2001).
[29]M. Strange and K. S. Thygesen, Phys. Rev. B **86**, 195121 (2012).
[30]S. Sharifzadeh, I. Tamblyn, P. Doak, P. T. Darancet, and J. B. Neaton, Eur. Phys. J. B **85**, 323 (2012).

[31]A. M. Souza, I. Rungger, C. D. Pemmaraju, U. Schwingenschloegl, and S. Sanvito, Phys. Rev. B **88**, 165112 (2013).

[32]R. Stadler, V. Geskin, and J. Cornil, Phys. Rev. B **78**, 113402 (2008).

[33]R. Stadler, V. Geskin, and J. Cornil, Phys. Rev. B **79**, 113408 (2009).

[34]C. J. O. Verzijl and J. M. Thijssen, J. Phys. Chem. C **116**, 24393 (2012).

[35]C. R. Jacob and M. Reiher, Int. J. Quantum Chem. **112**, 3661 (2012).

[36]J. P. Perdew, R. G. Parr, M. Levy, and J. L. Balduz, Phys. Rev. Lett. **49**, 1691 (1982).

[37]K. Burke, J. Chem. Phys. **136**, 150901 (2012).

[38]Z.-F. Liu, J. P. Bergfield, K. Burke, and C. A. Stafford, Phys. Rev. B **85**, 155117 (2012).

[39]J. P. Bergfield, Z.-F. Liu, K. Burke, and C. A. Stafford, Phys. Rev. Lett. **108**, 066801 (2012).

[40]Z.-F. Liu and K. Burke, Phys. Rev. B **91**, 245158 (2015).

[41]K. S. Thygesen and A. Rubio, Phys. Rev. Lett. **102**, 046802 (2009).

[42]Q. Wu and T. Van Voorhis, Phys. Rev. A **72**, 024502 (2005).

[43]Q. Wu and T. Van Voorhis, J. Chem. Theory Comput. **2**, 765 (2006).

[44]B. Kaduk, T. Kowalczyk, and T. Van Voorhis, Chem. Rev. **112**, 321 (2012).

[45]G. te Velde and E. J. Baerends, Phys. Rev. B **44**, 7888 (1991).

[46]G. Wiesenekker and E. J. Baerends, J. Phys.: Condens. Matter **3**, 6721 (1991).

[47]S. G. Lias, in *NIST Chemistry Webbook, NIST Standard Reference Database Number 69*, edited by P. J. Linstrom and W. G. Mallard (National Institute of Standards and Technology, Gaithersburg, MD, 2012), http://webbook.nist.gov.

[48]P. D. Burrow, J. A. Michejda, and K. D. Jordan, J. Chem. Phys. **86**, 9 (1987).

[49]V. M. García-Suárez and C. J. Lambert, New J. Phys. **13**, 053026 (2011).

[50]S. Y. Quek, H. J. Choi, S. G. Louie, and J. B. Neaton, Nano Lett. **9**, 3949 (2009).

[51]L. Venkataraman, J. E. Klare, C. Nuckolls, M. S. Hybertsen, and M. L. Steigerwald, Nature **442**, 904 (2006).

[52]M. Kiguchi, S. Miura, T. Takahashi, K. Hara, M. Sawamura, and K. Murakoshi, J. Phys. Chem. C **112**, 13349 (2008).